J|A|C|S
COMMUNICATIONS

Published on Web 03/16/2006

Aerosol-Assisted Self-Assembly of Single-Crystal Core/Nanoporous Shell Particles as Model Controlled Release Capsules

Xingmao Jiang and C. Jeffrey Brinker*

Department of Chemical and Nuclear Engineering and Center for Micro-Engineered Materials, University of New Mexico, Albuquerque, New Mexico 87106, and Sandia National Laboratories, Albuquerque, New Mexico 87185

Received December 5, 2005; E-mail: cjbrink@sandia.gov

Controlled release is a central theme of nano-engineering and is important to a wide spectrum of technologies ranging from drug delivery to corrosion inhibition.[1] Recently, several types of controlled release architectures have been developed based on incorporation of the release agent in nanoporous hosts.[2] In these constructs, silica/surfactant self-assembly allows precise control of the host pore size, and various gating strategies have been used to modulate the release characteristics.[3] However, as these systems are synthesized in batch reactors requiring multiple synthesis steps,[1−3] they may not be amenable to large-scale manufacturing. Here we describe a rapid, single step, aerosol-assisted self-assembly process to fabricate model core shell particles in which a single-crystal core is incorporated in a spherical nanoporous particle. The combined control of pore size and pore surface chemistry allows the characteristic release time to be varied by over 4 orders of magnitude. The use of a continuous aerosol reactor and principally aqueous solvents makes this green process suitable for industrialization.

In the aerosol-assisted self-assembly process,[4] alcohol/water solutions of soluble silica plus surfactant (and optionally other components) are prepared as aerosols and evaporated to form highly ordered hexagonal, cubic, or lamellar (vesicular) mesophase particles. Unlike the related evaporation-induced self-assembly (EISA) of films,[5] where gradients in composition develop along the film or through its thickness, EISA confined to spherical aerosol droplets results in radial concentration gradients, and self-assembly is accordingly radially directed from the outer liquid−vapor interface toward the interior. To achieve a solid, completely ordered particle, the developing mesophase must continually rearrange itself to accommodate the reduction in volume and liquid−vapor interfacial area resulting from solvent evaporation. This requires the developing mesophase to remain fluid throughout the course of self-assembly.

As a model system in which to study controlled release, we synthesized NaCl containing mesoporous particles via aerosol-assisted self-assembly using cetyltrimethylammoniumbromide (CTAB) as the structure directing agent and varying the silica precursor over the range of 100% tetraethoxysilane (TEOS) to 40%TEOS/60% methyltriethoxysilane (MTES) to adjust the wetting behavior of the pore surfaces. The process begins with a homogeneous precursor solution prepared as (molar ratios) 1 Si:9.9 EtOH: 63.3 water:0.022 HCl:0.22 CTAB:0.33 NaCl, where Si represents MTES/TEOS in the molar ratios 0/100, 10/90, 20/80, and 40/60, corresponding to samples A, B, C, and D, respectively. Aerosol droplets were generated using an atomizer (Model 9302A, TSI) operated with nitrogen as the carrier gas. The aerosol droplets (initial average diameter $< 10\ \mu$m) were dried, solidified in a tube furnace (maintained at 400 °C), and finally calcined at 400 °C for 5 h in argon (heating rate, 1 °C/min) to remove CTAB.

Figure 1A shows a representative bright field TEM image of sample A particles. Selected area electron diffraction (SAED) and dark field imaging (Figure 1B and 1C, respectively) indicate that

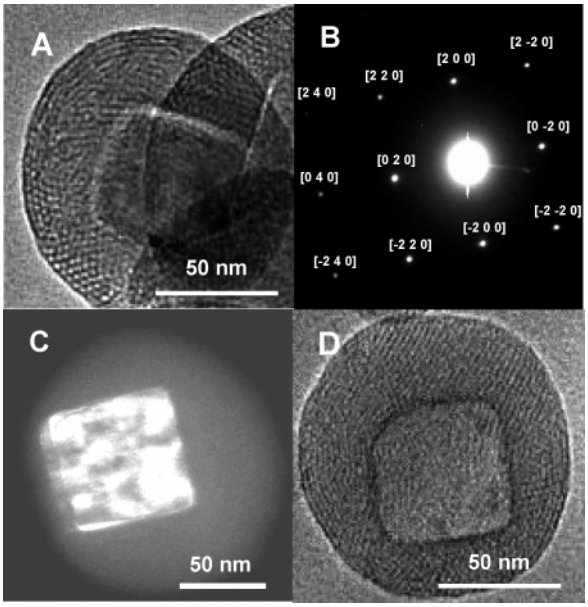

Figure 1. TEM images for nanostructured sample A particles. (A) Cubic single-crystal NaCl/hexagonally ordered mesoporous silica. (B) Selected area electron diffraction pattern (SAED) with a [0 0 1] zone. (C) Dark field image. (D) Silica particle after release in water.

the polyhedral core observed in Figure 1A is a single crystal of NaCl. A conformal, mesoporous silica shell surrounds the NaCl core. The mesostructural features at the particle perimeters are observed to be stripes aligned parallel to the particle perimeters or hexagonal arrangements of pores with pore centers aligned parallel to the particle perimeters—both features being consistent with differing orientations of a 2D hexagonal silica mesophase confined within a spherical shell. (Despite these arrangements, as shown below, the pores remain completely accessible to gas and liquid). The SAED pattern matches that of NaCl with zone axis [001]. The solid nature of the particles and conformity of the mesoporous silica shell to the single-crystal NaCl core for all the samples emphasize that the developing silica mesophase remains fluid throughout the course of aerosol-assisted self-assembly.

Figure S1 shows XRD patterns for samples A−D. Narrow high angle peaks observed are indexed as NaCl (*Fm*3*m*) with unit cell dimension of 5.640 Å. The low angle peaks are associated with the 2D hexagonal silica mesophase. With increasing MTES/TEOS ratios, the low angle diffraction peaks initially become narrower and more intense, indicating greater mesostructural order. This is opposite to the behavior observed for EISA of MTES/TEOS systems prepared without added NaCl. The increased ionic strength of the present systems screens electrostatic interactions, reducing the optimal CTAB headgroup area.[6] Up to a point, this may allow greater accommodation of amphiphilic hydrolyzed MTES at the silica/surfactant interface, while maintaining appropriate charge

10.1021/ja058260+ CCC: $33.50

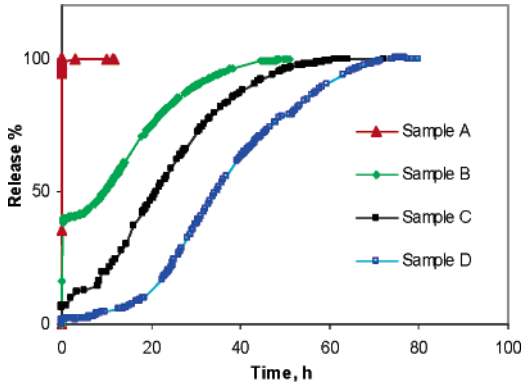

Figure 2. Release profiles for samples A, B, C, and D.

density matching.[7] At the highest MTES/TEOS ratio investigated, the mesostructural order is reduced as measured by broadened and less intense diffraction peaks. Regardless of the extent of mesostructural order, all four samples exhibit Type IV nitrogen adsorption−desorption isotherms (Figure S5) having no hysteresis, as is typical of hexagonal MCM-41-like mesoporous silicas.[8] With increasing MTES/TEOS ratios, the average Barrett−Joyner−Halenda (BJH) pore size decreased from 2.06 to 1.50 nm, corresponding to progressively greater occlusion of the pore channels as OH groups are replaced with CH_3 groups. The increasing ratios also increase surface hydrophobicity. Films of particles prepared by dispersing the particles in hexane and spin-coating exhibited (apparent) static water contact angles of 50, 57, 70, and 103° for samples A−D, respectively. Greater hydrophobicity also improves the hydrothermal stability—sample D shows no change in BET surface area or BJH pore size after 12 h in 100 °C water.

We investigated the release behaviors of the samples dispersed in deionized water by measurements of the ionic conductivity at 25 °C. As shown in Figure 2, with increasing MTES/TEOS, release times increase from several seconds to 80 h. Sample A prepared exclusively with hydrophilic Si−OH-terminated pore surfaces exhibits immediate rapid release, presumably due to rapid water infiltration and high ionic diffusivities in the 2 nm mesoporous channels (D evaluated by the Crank−Nicholson numerical method $= 2.5 \times 10^{-13}$ m^2 s^{-1}). By comparison, all the MTES-containing samples exhibit S-shaped curves with an induction time that increases with MTES content, presumably due to delayed capillary filling of the mesopores (filling rate scales with cos θ). For all samples, complete NaCl release creates a hollow cubic cavity at the particle core (Figure 1D).

The single-crystal core/mesoporous shell architecture of our particles is principally a consequence of the radial concentration gradients established during drying of multicomponent spherical droplets and their influence on surfactant/silica self-assembly, ionic solubility, and crystal nucleation and growth. Numerical solutions to the radial gradients in mass and heat for evaporating 10 μm diameter H_2O−ethanol−NaCl droplets, with initial temperature of 70 °C and initial composition similar to that of samples A−D (excluding silica and surfactant), indicate that preferential ethanol evaporation enriches the droplet surface in water. As NaCl is 481 times more soluble in water than in ethanol (25 °C), and the ionic diffusivity of Na^+ and Cl^- exceeds that of both water and ethanol, supersaturation of Na^+ and Cl^- and nucleation of NaCl occur first at the particle center, where the EtOH/H_2O ratio is maximized. The rather large stable nucleus size for NaCl and small droplet size require that, once a single stable nucleus forms, the remainder of the droplet becomes substantially depleted in Na^+ and Cl^-, reducing the probability of multiple nucleation events. Further, if multiple nuclei were to form, the high water solubility and high diffusivity of Na^+ and Cl^- enforce the conditions for Oswald ripening, the preferential dissolution of smaller crystallites and growth of larger, more stable crystals driven by their differential solubilities.

The concurrent mesophase self-assembly process depends on the concentration gradients of the nonvolatile silica and surfactant components. It initiates, therefore, on the droplet surface, where the critical micelle concentration is first exceeded, and proceeds inward with a longer time scale characteristic of the drying process. Although the evolving silica/surfactant mesophase remains fluid throughout the course of self-assembly, allowing accommodation of the diminishing droplet volume and interfacial area, it is expected that the high viscosity of these associated assemblies suppresses large-scale diffusivity, and the mesophase develops radially toward the particle interior. The conformity of the silica/surfactant mesophase to the single-crystal core and apparent absence of silica in the core suggest that the NaCl single-crystal core forms before self-assembly of the shell. However, as is known for crystal growth in silica gels, a growing crystal[9,10] can displace and deform a gel, and the same is expected for the fluid silica/surfactant mesophase studied here.

We have shown a simple, rapid process to create novel single-crystal core/mesoporous shell nanoparticles. This architecture depends on radial concentration gradients that develop naturally in evaporating droplets along with high ionic diffusivity and high differential ionic solubility in the binary solvent system. As such, with judicious choice of solute and solvent, it should be extendable to other systems of interest for controlled release.

Acknowledgment. This work was supported by NSF NIRT, AFOSR, DOE, and ARO. Sandia is operated for U.S. DOE under Contract DE-AC04-94AL85000.

Supporting Information Available: Figures S1−S6 and experimental details (PDF). This material is available free of charge via the Internet at http://pubs.acs.org.

References

(1) (a) Nguyen, T. D.; Tseng, H. R.; Celestre, P. C.; Flood, A. H.; Liu, Y.; Stoddart, J. F.; Zink, J. I. *Proc. Natl. Acad. Sci. U.S.A.* **2005**, *102*, 10029. (b) Trewyn, B. G.; Whitman, C. M.; Lin, V. S. Y. *Nano Lett.* **2004**, *4*, 2139.
(2) (a) Zhao, D. Y.; Yang, P. D.; Chmelka, B. F.; Stucky, G. D. *Chem. Mater.* **1999**, *11*, 1174. (b) Lai, C. Y.; Trewyn, B. G.; Jeftinija, D. M.; Jeftinija, K.; Xu, S.; Jeftinija, S.; Lin, V. S. Y. *J. Am. Chem. Soc.* **2003**, *125*, 4451. (c) Vallet-Regi, M.; Doadrio, J. C.; Doadrio, A. L.; Izquierdo-Barba, I.; Perez-Pariente, J. *Solid State Ion.* **2004**, *172*, 435. (d) Li, Z. Z.; Wen, L. X.; Shao, L.; Chen, J. F. *J. Controlled Release* **2004**, *98*, 245.
(3) (a) Gruenhagen, J. A.; Lai, C. Y.; Radu, D. R.; Lin, V. S. Y.; Yeung, E. S. *Appl. Spectrosc.* **2005**, *59*, 424. (b) Tan, B.; Rankin, S. E. *Langmuir* **2005**, *21*, 8180. (c) Mal, N. K.; Fujiwara, M.; Tanaka, Y.; Taguchi, T.; Matsukata, M. *Chem. Mater.* **2003**, *15*, 3385.
(4) Lu, Y. F.; Fan, H. Y.; Stump, A.; Ward, T. L.; Rieker, T.; Brinker, C. J. *Nature* **1999**, *398*, 223.
(5) Lu, Y. F.; Ganguli, R.; Drewien, C. A.; Anderson, M. T.; Brinker, C. J.; Gong, W. L.; Guo, Y. X.; Soyez, H.; Dunn, B.; Huang, M. H.; Zink, J. I. *Nature* **1997**, *389*, 364.
(6) Chiruvolu, S.; Israelachvili, J. N.; Naranjo, E.; Xu, Z.; Zasadzinski, J. A.; Kaler, E. W.; Herrington, K. L. *Langmuir* **1995**, *11*, 4256.
(7) Monnier, A.; Schuth, F.; Huo, Q.; Kumar, D.; Margolese, D.; Maxwell, R. S.; Stucky, G. D.; Krishnamutry, M.; Petroff, P.; Firouzi, A.; Janicke, M.; Chmelka, B. F. *Science* **1993**, *261*, 1299.
(8) Kruk, M.; Jaroniec, M.; Sayari, A. *Langmuir* **1997**, *13*, 6267.
(9) Nishihara, H.; Mukai, S. R.; Yamashita, D.; Tamon, H. *Chem. Mater.* **2005**, *17*, 683.
(10) Mahler, W.; Bechtold, M. F. *Nature* **1980**, *285*, 27.

JA058260+